applied sciences

MDPI

Article

Influence of Operating Parameters on Photocatalytic Oxidation of 2,4-Dichlorofenol in Aqueous Solution by TiO_2/Stainless Steel Photocatalytic Membrane

Liliana Bobirică, Constantin Bobirică, Giovanina Iuliana Lupu and Cristina Orbeci *

Department of Analytical Chemistry and Environmental Engineering, University Politehnica of Bucharest, 1-7 Polizu, 011061 Bucharest, Romania; l_bobirica_ro@yahoo.com (L.B.); c_bobirica@yahoo.com (C.B.); giovanina.lupu@yahoo.com (G.I.L.)
* Correspondence: cristina.orbeci@upb.ro; Tel.: +40-721259875

Abstract: The influence of some operating parameters of an UV photocatalytic reactor with TiO_2/stainless steel photocatalytic membrane on the photocatalytic oxidation of 2,4-dichlorophenol from aqueous solutions was studied in this paper. It was shown that the pH of the working solution substantially influences the photocatalytic degradation of the organic substrate, with the degradation efficiency increasing with decreasing the pH of the working solution by a maximum corresponding to pH 3. The rate constant of the photocatalytic oxidation process is about twice as high at pH 3 comparative with pH 7 for the same initial concentration of the organic substrate. The molar ratio of hydrogen peroxide/organic substrate also influences the photocatalytic oxidation process of the organic substrate. The results obtained in this paper highlight the fact that a stoichiometric molar ratio is favorable for the photocatalytic degradation of 2,4-dichlorophenol. It has also been shown that the initial concentration of the organic substrate influences the rate of photocatalytic degradation. It appears that the rate of photocatalytic degradation decreases with the increasing of initial concentration of 2,4-dichlorophenol.

Keywords: photocatalytic oxidation; chlorophenols; photocatalytic membrane; titanium dioxide

Citation: Bobirică, L.; Bobirică, C.; Lupu, G.I.; Orbeci, C. Influence of Operating Parameters on Photocatalytic Oxidation of 2,4-Dichlorofenol in Aqueous Solution by TiO_2/Stainless Steel Photocatalytic Membrane. *Appl. Sci.* **2021**, *11*, 11664. https://doi.org/10.3390/app112411664

Academic Editors: Cseh Liliana, Florica Manea, Tudose Ramona and Szerb Elisabeta Ildyko

Received: 23 November 2021
Accepted: 6 December 2021
Published: 9 December 2021

1. Introduction

The rapid development of various industrial sectors around the world has recently led to an increase in the diversity of pollutants that reach natural water bodies. Many of these pollutants cannot be removed naturally from these waters. Therefore, they have a long residence time and can have a serious long-term negative effect on these natural systems [1,2]. A significant category of these persistent pollutants is represented by refractory organic compounds, which include chlorophenols. They end up in wastewater resulting from the manufacture of pesticides, paints, polymers, cosmetics, etc., and because they cannot be removed by conventional methods in wastewater treatment plants, they arrive in natural water bodies [3,4].

2,4-dichlorophenol is one of the most toxic chlorophenols with a major negative impact on aquatic life and human health and, therefore, is classified as a priority pollutant in the United States of America (USA) and European Union (EU) [5]. It is also persistent and bioaccumulative in the environment, being suspected of producing carcinogenic and mutagenic effects on living organisms [6]. The World Health Organization (WHO) has set a maximum allowable concentration of 0.1 µg/L in drinking water and 1 mg/L in treated wastewater discharged into natural water bodies [7].

Photochemical advanced oxidation processes are the most widely used methods for wastewater treatment containing refractory organic compounds. Of these, the most popular seems to be the photocatalytic oxidation [8,9]. Titanium dioxide is the most used photocatalyst due to its advantages such as high stability, low toxicity, availability,

low cost, and low environmental adversity [10]. The photocatalyst can be immobilized in the photocatalytic reactor (either by depositing it on a membrane, by adding it to a membrane, or by making a stand-alone photocatalyst membrane), or it can be dispersed in the aqueous solution to be treated. It has been shown that each option to configure the photocatalytic reactor has both advantages and disadvantages depending on the specific application [11]. For example, photocatalytic reactors with dispersed photocatalysts usually have the main advantage of a larger active surface area which generally gives them a higher substrate degradation efficiency than photocatalytic reactors with immobilized photocatalysts. Instead, this type of photocatalytic reactor has the major disadvantage of the need to separate the photocatalyst from the suspension and reuse it [12–15]. At the same time, photocatalytic reactors with immobilized photocatalyst have, among other things, the great advantage of the possibility of being operated continuously, at least for the time interval in which the membrane has sufficient photocatalytic activity. Regeneration of photocatalytic membranes is usually much easier to achieve compared to dispersed photocatalysts [16–19].

However, regardless of the reactor configuration, the photocatalytic activity of the system largely depends on its operating parameters, such as the initial organic substrate concentration, photocatalyst loading, photocatalytic reactor and photocatalytic membrane geometry, the physico-chemical characteristics of the aqueous solution subjected to the treatment, light wavelength and its intensity, etc. Despite the many studies conducted in this field that have led to significant achievements, there are still many problems that need to be solved, especially for specific applications and photocatalytic systems designed to work on an industrial scale [20].

Usually, the efficiency of removing the refractory organic material from aqueous solutions depends on the particularities of the photocatalytic system used [21]. For example, studies on TiO_2-based UV photocatalytic degradation of 2,4-dichlorophenol have shown that the efficiency of removing refractory organic material from aqueous solutions as a function of its initial pH differs from one photocatalytic system to another. Thus, it was found that for a photocatalytic system with dispersed TiO_2, the photocatalytic degradation efficiency is maximum at a pH of the aqueous solution of 5 [22]. For a photocatalytic system with dispersed TiO_2 intercalated talc nanocomposite, the best results were recorded for neutral conditions of the aqueous solution of 2,4-dichlorophenol [23]. In the case of a photocatalytic system with dispersed Fe/TiO_2, the maximum degradation efficiency of 2,4-dichlorophenol in aqueous solution was recorded at a pH of 4 [24]. For a photocatalytic system with a Fe^0/TiO_2/ACF (activated carbon fiber) composite photocatalytic membrane, it has been established that the optimum pH of the aqueous 2,4-dichlorophenol solution subjected to the photocatalytic treatment is 6 [25]. Thus, it becomes clear that for each new photocatalytic system, it is necessary to optimize the operating parameters in order to obtain the highest possible photocatalytic degradation efficiency of specific refractory organic compounds.

Therefore, the influence of some operating conditions on the performances of an UV photocatalytic reactor with an immobilized photocatalyst (new photocatalytic membrane —titanium dioxide deposited on the stainless-steel grid support, TiO_2/stainless steel) for removing 2,4-dichlorophenol from aqueous solutions was studied in this work. The paper aims to identify the optimal pH of the working solution and to establish the need for hydrogen peroxide to be added to the system so that the efficiency of photocatalytic degradation is as high as possible. The influence of the initial concentration of the organic substrate is also investigated.

2. Materials and Methods

2.1. Materials and Reagents

2,4-dichlorophenol ($C_6H_4Cl_2O$) used in experiments as an organic substrate was of analytical grade and was purchased from Fluka Chemicals. In the text of the paper, the acronym 2,4-DCF will be used for this reagent. Hydrogen peroxide (H_2O_2) solution 30%

by mass was purchased from Sigma-Aldrich, and it was used as a source of hydroxyl radical species. A solution of 1 N (normality) sulfuric acid (H_2SO_4) purchased from Sigma-Aldrich was used to adjust the pH of the working solutions to the default values. Chemical oxygen demand (COD) analysis was performed by using potassium dichromate ($K_2Cr_2O_7$), mercuric sulfate ($HgSO_4$), silver sulfate (Ag_2SO_4), potassium acid phthalate ($C_8H_5KO_4$), as well as sulfuric acid 95–97% by mass, all of them of analytical grade purchased from Sigma-Aldrich. Distilled water was used to prepare all reagent and working solutions. The photocatalytic membrane is made from a stainless-steel grid support (cylindrical shape, 10 cm × 30 cm) on which TiO_2 (P25 from Degussa, Essen, Germany) was deposited by electrophoretic deposition.

2.2. Dark Adsorption Experiments

Dark adsorption experiments were performed under same conditions with photocatalytic degradation experiments but without putting into operation the UV lamp of the photocatalytic reactor (without UV radiation) and without addition of hydrogen peroxide. In this respect, a UV photocatalytic reactor with photocatalytic membrane was used in which the working solution was continually recirculated through a recirculation vessel by means of an external centrifugal pump. The photocatalytic reactor is designed so that the UV lamp, the photocatalytic membrane, and the water-cooling jacket are coaxially positioned inside it. The characteristics and operating parameters of the photocatalytic reactor are presented in Table 1.

Table 1. Photocatalytic experimental conditions.

Reactor Volume, L	1.5
2,4-DCF working solution volume, L	2
Recirculation flow rate, L/min	1
UV lamp	High-pressure mercury lamp; power: 120 W; wavelength peak: 365 nm; peak irradiance (intensity): 1.5 mW/cm^2; energy density (dose for 2 h of irradiance): 10.8 J/cm^2
2,4-DCF working solution pH	2, 3, 5, and 7
Hydrogen peroxide/2,4-DCF molar ratio	0.5, 1, and 2
Membrane	TiO_2/stainless steel

In the case of experiments on adsorption isotherms, working solutions were prepared with the initial COD equivalent concentration of 2,4-DCF ranging from 50 to 300 mg O_2/L. It should be mentioned that because in photocatalytic experiments it is more useful to report the content in organic substrate in terms of organic carbon (OC), throughout this work the content in organic substrate is expressed exclusively in terms of organic carbon. Thus, for adsorption isotherms experiments the organic carbon equivalent initial concentrations of 2,4-DCF solutions ranged from 18.75 to 112.50 mg OC/L. After the solutions were prepared, their pH was adjusted to the default values (pH of 2, 3, 5, and 7). Next, each working solution was introduced in the photocatalytic reactor, and by means of the external centrifugal pump these were recirculated at room temperature until the equilibrium concentration was reached. The samples by which the adsorption equilibrium was checked were taken from the photocatalytic reactor by means of its special sampling holes without the need to turn it off. Next, the samples were prepared and measured for their organic content by COD analysis following the APHA 5220 D standard method [26]. Both LT 200 thermostat and DR 3800 spectrophotometer (Hach Lange GmbH, Weinheim, Germany) were used to carry out the analysis. Regeneration of the photocatalytic membrane was accomplished by operating the reactor charged with distilled water to which oxygen peroxide was added for two hours in the presence of UV radiation. The regeneration procedure was applied

after each experiment. The amount of 2,4-DCF adsorbed on the photocatalytic membrane was established based on Equation (1).

$$q_{eq} = \frac{(C_0 - C_{eq})V}{m} \quad (1)$$

where q_{eq} is the amount of 2,4-DCF adsorbed on the photocatalytic membrane at equilibrium (mg/g), V is the volume of the working solution (L), C_0 and C_{eq} are the initial and equilibrium concentration of 2,4-DCF (mg/L), and m is the mass of the photocatalytic membrane (g). The adsorption isotherms were plotted in terms of the amount of 2,4-DCF adsorbed (expressed as organic carbon) on the photocatalytic membrane q_{eq} (mg/g) against of equilibrium concentration of 2,4-DCF C_{eq} (mg/L).

The experiments on adsorption kinetics were performed in the same way as those on adsorption isotherms. For these experiments, working solutions were prepared with initial COD equivalent concentration of 2,4-DCF of 100, 200, and 300 mg O_2/L. Thus, the organic carbon equivalent initial concentrations of 2,4-DCF solutions were 37.50, 75.00, and 112.50 mg OC/L. The amount of 2,4-DCF adsorbed on the photocatalytic membrane was determined was established based on Equation (2).

$$q_t = \frac{(C_0 - C_t) \times V}{m} \quad (2)$$

where q_t is the amount of 2,4-DCF adsorbed on the photocatalytic membrane at time t (mg/g), V is the volume of the working solution (L), C_0 and C_t are the initial and residual concentration of 2,4-DCF at time t (mg/L), and m is the mass of the photocatalytic membrane (g). A pseudo-second-order kinetic model was used to evaluate the experimental data for adsorption kinetics.

2.3. Photocatalytic Oxidation Experiments

The photocatalytic degradation was conducted by monitoring the evolution of the organic content of the working solution as a function of irradiation time. Thus, samples of about 10 mL were taken from reactor at predetermined irradiation times. After the solutions were prepared, their pH was adjusted to the default value and the calculated amount of hydrogen peroxide was added. Further, the experiments were performed similar to the previous ones, except that the UV lamp was turned on. The experimental conditions are presented in Table 1.

3. Results

3.1. Dark Adsorption Experiments

3.1.1. Adsorption Isotherms

The adsorption isotherms obtained for 2,4-DCF-TiO_2/stainless steel system for the four pH values of the working solution are presented in Figure 1. To describe the types of interactions between the adsorbate (2,4-DCF) and the adsorbent (TiO_2/stainless steel membrane), and to determine the maximum adsorption capacity of the adsorbent, Langmuir (Equation (3)) and Freundlich (Equation (4)) isotherm models were used [27]. The parameters of the adsorption process are presented in Table 2. As can be seen, the pH value of the working solution influences the adsorption process, the adsorption capacity at pH 3 being about 13% higher than at pH 7. The slight decrease of the adsorption capacity at pH 2 could be attributed to the increase of the instability of the photocatalytic membrane in strong acidic conditions (i.e., formation of titanium hydroxo complexes with hydroxyl ions release) which leads to the modification of the properties of the aqueous environment in which the adsorption takes place.

$$\frac{C_e}{q_e} = \frac{1}{K_L} + \frac{C_e}{q_m} \quad (3)$$

$$q_e = K_F \times C_e^{1/n} \quad (4)$$

where q_e is the adsorption capacity at equilibrium (mg 2,4-DCF/g of adsorbent), K_L is the Langmuir adsorption constant (L/mg), K_F is the Freundlich adsorption constant ($mg^{1-n} \cdot L^n/g$) related to the energy of adsorption, C_e is the equilibrium concentration of 2,4-DCF in the aqueous solution (mg/L), q_m is the maximum adsorption capacity (mg 2,4-DCF/g of adsorbent) and 1/n is the heterogeneity factor (dimensionless).

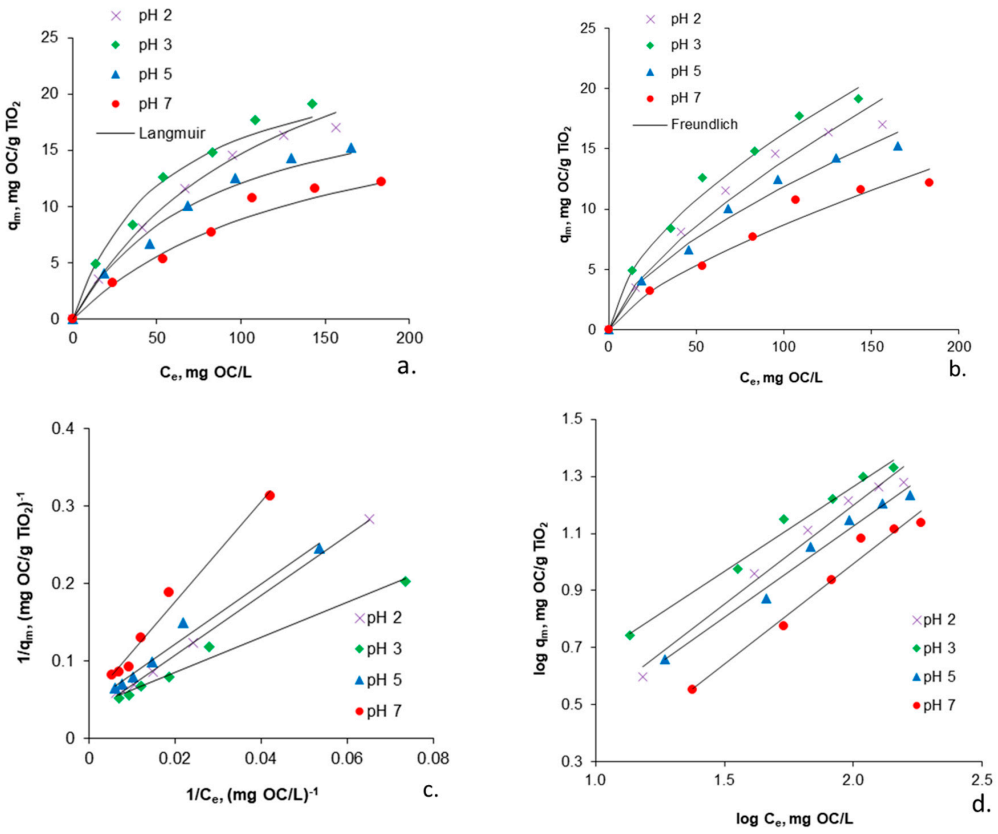

Figure 1. Adsorption isotherms of 2,4-DCF (expressed as OC) from aqueous solutions in different pH conditions: (**a**) non-linear fitting of Langmuir isotherm; (**b**) non-linear fitting of Freundlich isotherm; (**c**) linear fitting of Langmuir isotherm; (**d**) linear fitting of Freundlich isotherm.

Table 2. Fitting parameters for 2,4-DCF adsorption on TiO_2/stainless steel photocatalytic membrane.

pH	Langmuir			Freundlich		
	K_L (L/mg)	q_{mmax} (mg/g)	R^2	K_F ($mg^{1-n} \cdot L^n/g$)	n	R^2
2	0.016	23.568	0.9984	0.87	1.61	0.9794
3	0.018	24.876	0.9822	1.05	1.68	0.9865
5	0.012	22.173	0.9784	0.62	1.56	0.9826
7	0.007	21.598	0.9818	0.34	1.42	0.9727

The value of parameter n in the Freundlich model provides information on the average adsorption energy. If n has values less than 1, the interactions between adsorbent and adsorbate are weak, and if n is greater than 1 the interactions are strong. At values of n equal to 1 it is assumed that all active centers are similar in terms of energy, and the experimental data fit better on the theoretical curves obtained with the Langmuir model. In this respect, as can be seen for all working conditions, the parameter n has values above 1 which suggests that there is a strong interaction between 2,4-DCF and the adsorbent, but the number of heterogeneous active centers is limited. Therefore, this is also the reason why the experimental data fit better on the Langmuir isotherm. It can also be seen that

the value of parameter n increases with the decrease of the pH of the working solution which indicates that the interactions between the adsorbent and chlorophenol are stronger in acidic medium.

The analysis of the adsorption parameters obtained with Langmuir model provides a similar image to the one outlined in the analysis of the adsorption parameters obtained with the Freundlich model. Thus, the values of the maximum adsorption capacity q_{mmax} and of the Langmuir adsorption constant (K_L) increase with the decrease of the pH values of the working solution with a maximum corresponding to pH 3. Because the Langmuir adsorption constant provides information on the binding energy between the adsorbent and the adsorbate, increasing its values as the pH of the working solution decreases indicates that the binding energy between chlorophenol and the adsorbent is higher in acidic aqueous solutions.

3.1.2. Adsorption Kinetics

The adsorption kinetics for 2,4-DCF-TiO_2/stainless steel system for the four pH values of the working solution is presented in Figure 2 (non-linear fitting) and Figure 3 (linear fitting). It is observed that the adsorption process proceeds rapidly, the adsorption equilibrium being reached after about 30 min regardless of the initial concentration of 2,4-DCF. The pH of the working solution influences the adsorption capacity of the photocatalytic membrane in the sense that for the same initial concentration of 2,4-DCF there is an increase in the adsorption capacity of the catalyst as the pH of the working solution decreases with a maximum corresponding to pH 3. Thus, for an initial concentration of 2,4-DCF of 84.9 mg/L the adsorption capacity of the catalyst increases from 5.311 mg 2,4-DCF/g adsorbent at pH 7 to 8.413 mg 2,4-DCF/g adsorbent at pH 3, for an initial concentration of 169.79 mg/L the adsorption capacity of the catalyst increases from 10.739 mg 2,4-DCF/g adsorbent at pH 7 to 14.803 mg 2,4-DCF/g adsorbent at pH 3, and for an initial concentration of 254.69 mg/L the adsorption capacity of the catalyst increases from 12.190 mg 2,4-DCF/g adsorbent at pH 7 to 19.156 mg 2,4-DCF /g adsorbent at pH 3.

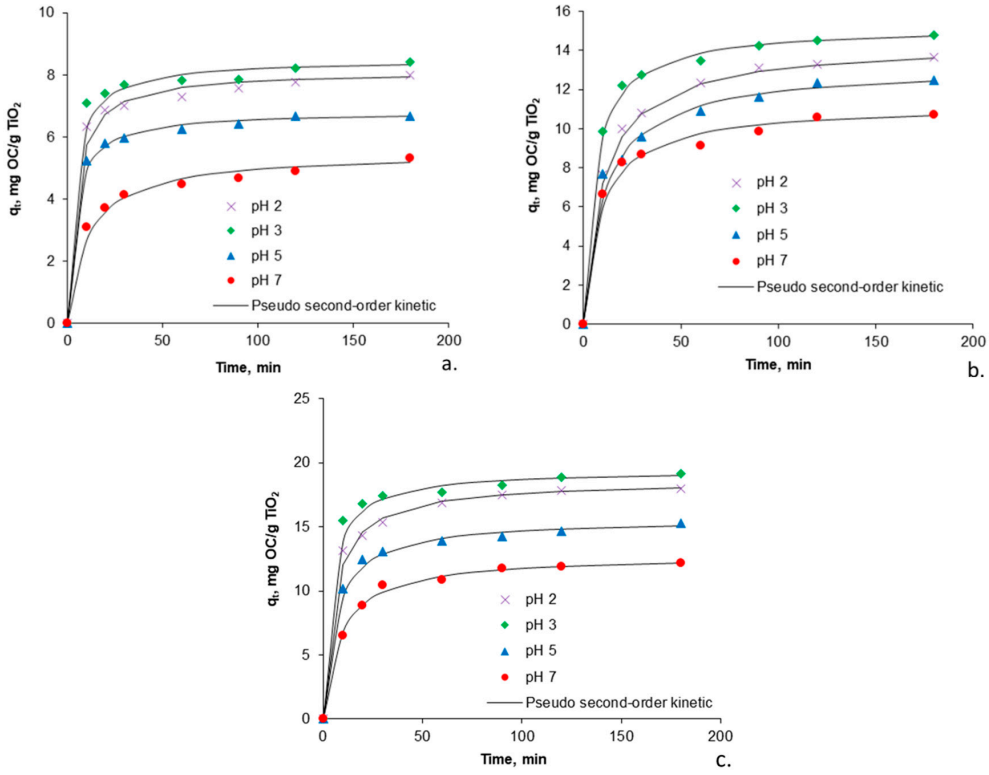

Figure 2. Adsorption kinetics of 2,4-DCF (expressed as OC) from aqueous solutions under different pH conditions and different initial concentrations: (**a**) 37.50 mg OC/L; (**b**) 75.00 mg OC/L; (**c**) 112.50 mg OC/L.

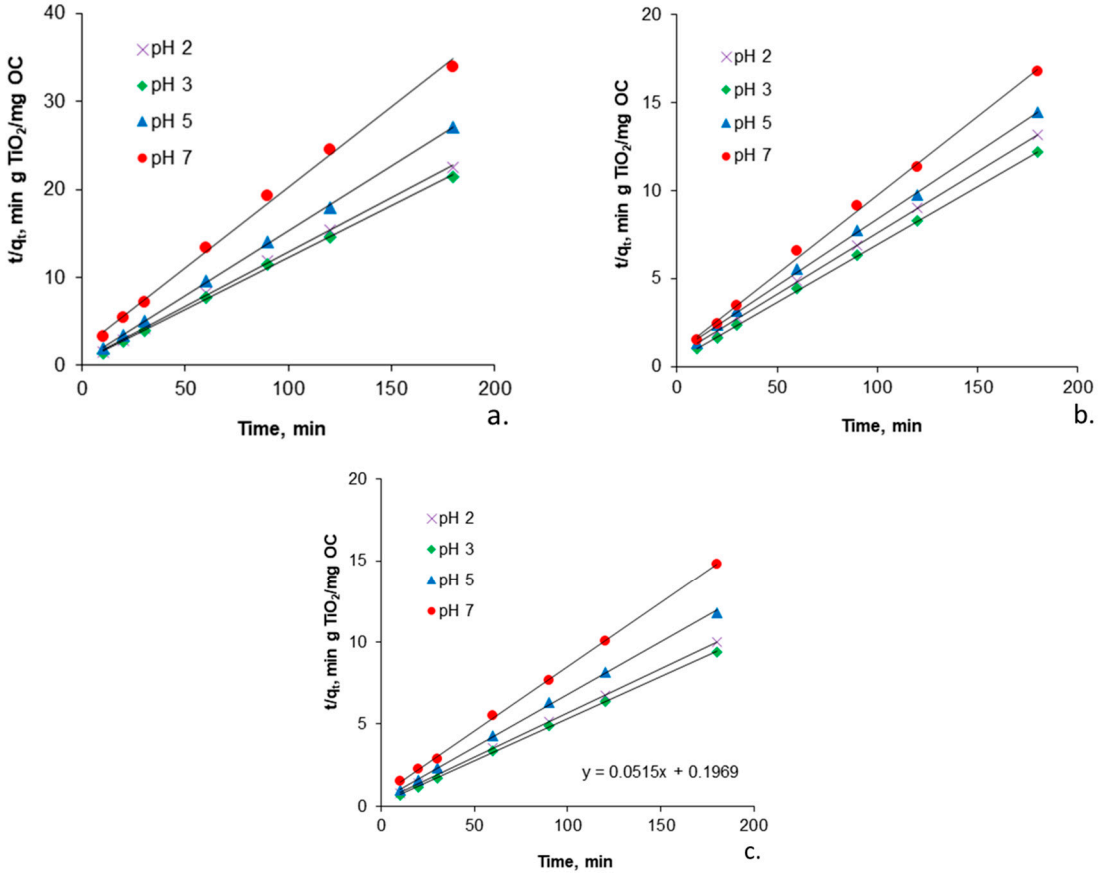

Figure 3. Linear fitting of adsorption kinetics of 2,4-DCF (expressed as OC) from aqueous solutions under different pH conditions and different initial concentrations: (**a**) 37.50 mg OC/L; (**b**) 75.00 mg OC/L; (**c**) 112.50 mg OC/L.

Second-order kinetics described by the equations presented below were used to estimate the kinetic parameters of the 2,4-DCF adsorption process [28]. The kinetic parameters and the correlation coefficients are presented in Table 3.

$$\frac{dq_t}{dt} = k(q_e - q_t)^2 \quad (5)$$

where q_t is the adsorption capacity of the adsorbent at time t, q_e represents the adsorption capacity of the adsorbent at equilibrium, and k represents the second order kinetic constant of the adsorption process, $g \cdot mg^{-1} \cdot min^{-1}$. The integrated form of the above equation (considering the boundary conditions t = 0, t = t and $q_t = 0$ $q_t = q_e$) is as follows:

$$\frac{1}{(q_e - q_t)} = \frac{1}{q_e} + kt \quad (6)$$

Rearranging the above equation, its linearized form is obtained:

$$\left(\frac{t}{q_t}\right) = \frac{1}{kq_e{}^2} + \frac{1}{q_e}(t) \quad (7)$$

$$h = kq_e{}^2 \quad (8)$$

$$t_{1/2} = \frac{1}{kq_e} \quad (9)$$

where h is the initial adsorption rate, $mg \cdot g^{-1} \cdot min^{-1}$, and $t_{1/2}$ represents the half-life, min. Representing graphically t/q_m as a function of t, a line is obtained from which q_e, k, h,

and $t_{1/2}$ can be calculated from the slope, respectively, the line at its origin. Regarding the kinetic parameters of the adsorption process, namely the initial adsorption rate and the half-life, their values vary depending on the pH value of the working solution. Thus, the initial adsorption rate increases as the pH of the working solution decreases, and the half-life decreases as the pH of the working solution decreases. These results suggest that in addition to increasing the adsorption capacity of the catalyst as the pH of the working solution decreases, the rate of the adsorption process and therefore its overall efficiency also increases. It should be noted that this trend is maintained until a pH of the working solution of 3. At lower pH values, this trend appears to change slightly, most likely due to decreased photocatalytic membrane stability in a strongly acidic environment.

Table 3. Fitting parameters for pseudo-second-order kinetics of 2,4-DCF adsorption on TiO_2/stainless steel photocatalytic membrane.

pH	Initial Concentration, mg OC/L											
	37.50				75.00				112.5			
	k [1]	q_e [2]	h [3]	$t_{1/2}$ [4]	k	q_e	h	$t_{1/2}$	k	q_e	h	$t_{1/2}$
2	0.033	8.120	2.176	3.732	0.010	14.347	2.058	6.993	0.009	18.553	3.098	5.988
3	0.037	8.489	2.666	3.185	0.011	15.244	2.556	5.952	0.013	19.417	4.901	3.968
5	0.023	6.807	1.066	6.410	0.009	13.193	1.566	8.403	0.008	15.601	1.947	8.000
7	0.017	5.485	0.512	10.753	0.007	11.186	0.876	12.820	0.005	12.788	0.818	15.625

[1] ($g \cdot mg^{-1} \cdot min^{-1}$); [2] (mg/g); [3] ($mg \cdot g^{-1} \cdot min^{-1}$); [4] (min).

The kinetic and thermodynamic results regarding the adsorption of 2,4-DCF on the TiO_2/stainless steel photocatalytic membrane show that the efficiency of the adsorption process increases with the increase of the acidity of the working solution with a maximum corresponding to pH 3. This result is highlighted in Figure 4. As can be seen, simultaneously with the decrease of the adsorption process efficiency with the decrease of the acidity of the working solution there is also a decrease of the adsorption process efficiency with the increase of the initial chlorophenol concentration. The low efficiency recorded in all cases can be attributed to the fact that the adsorbent (TiO_2 catalyst) is deposited on a stainless-steel support in the form of a grid and is not suspended, with the specific surface in this case being smaller.

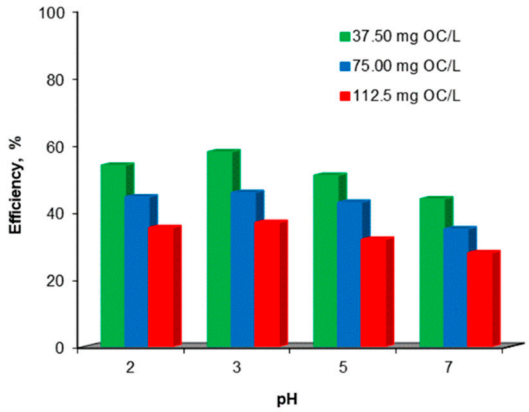

Figure 4. Adsorption efficiency of 2,4-DCF from aqueous solutions under different pH conditions and different initial concentrations.

3.2. Kinetics of Photocatalytic Oxidation

Because the photocatalytic oxidation process mainly involves two stages, one of adsorption of the organic compound on the catalyst surface and another of photocatalytic oxidation itself, the experimental results were interpreted based on the Langmuir–Hinshelwood (L-H) model which takes into account these two main stages. The Langmuir–

Hinshelwood (L-H) model was initially used to quantitatively describe solid–gas reactions. Currently the Langmuir-Hinshelwood model is also used to describe the kinetics of reactions that take place in the solid–liquid system by a rate law in which the reaction rate (r) is directly proportional to the fraction of surface area occupied by the substrate (θ) [29,30]:

$$r = -dC/dt = k\theta \quad (10)$$

Considering the form of the Langmuir equation:

$$\theta = KC/(1 + KC) \quad (11)$$

and substituting in the above equation obtains:

$$r = -dC/dt = k\theta = kKC/(1 + KC) \quad (12)$$

where k represents the rate constant, which is influenced by several parameters including catalyst mass, photon flux, etc. K represents the Langmuir–Hinshelwood equilibrium adsorption constant. Usually, the value of K is obtained from the Langmuir equation from kinetic studies performed in the presence of light, the results being much better than those obtained from studies in the dark. C represents the concentration of the organic substrate at time t. By integration, the above equation becomes:

$$\ln(C_0/C) + K(C_0 - C) = kKt \quad (13)$$

where C_0 represents the initial concentration of the organic substrate, and t represents the irradiation time. Equation (13) is considered to be of pseudo-zero order (Equation (14)) when the substrate concentration is high (>5×10^{-3} mol/L), and the reaction rate will be maximum. In the case of diluted solutions, the substrate concentration is low (<10^{-3} mol/L), and the reaction becomes apparently of pseudo-first order (Equation (15)).

$$(C_0 - C) = kt \quad (14)$$

$$-\frac{dC}{dt} = k_{ap}C \quad (15)$$

The linearized form of the above equation is described by the equation:

$$\ln\frac{C_0}{C} = k_{ap}t \quad (16)$$

$$t_{1/2} = \ln\frac{2}{k_{ap}} \quad (17)$$

By graphically representing the term ln (C_0/C) as a function of the irradiation time t, a line is obtained whose slope represents the apparent rate constant, k_{ap}. Its value can be used to calculate the half-life $t_{1/2}$. By the graphical representation of the term ln (C_0-C) as a function of short irradiation times, it is possible to identify the area in which the reaction takes place after a kinetics of pseudo-zero order. By multiplying the apparent rate constant k_{ap} obtained from the slope of the graph ln (C_0/C) as a function of the irradiation time with the initial concentration of organic substrate C_0, the value of the initial reaction rate r_0 is obtained for pseudo-first-order kinetics. This value can be used for comparison with other values of reaction rates obtained under various experimental conditions. After finding the value of the initial reaction rate, the values of the rate constant k and the adsorption constant K can be calculated using the model L-H described by an equation of the form:

$$r_0 = -dC/dt = kKC_0/(1 + KC_0) \quad (18)$$

$$1/r_0 = 1/kK \cdot 1/C_0 + 1/k \quad (19)$$

3.2.1. Influence of pH of the Working Solution

The initial rate values were calculated according to the methodology described above and were plotted as a function to the initial concentration of 2,4-DCF expressed in terms of organic carbon (Figure 5a) for the four pH values of the working solution. To determine the kinetic parameters, the linearized form of the Langmuir–Hinshelwood model was used (Figure 5b). Figure 5b shows that for all pH values in the chosen concentration range (18.5–112.5 mg OC/L), there is a linear dependence characterized by regression coefficients with values close to unity. Table 4 shows the values of the kinetic parameters obtained for the three pH values of the working solution at a hydrogen peroxide/chlorophenol molar ratio (N) of 1.

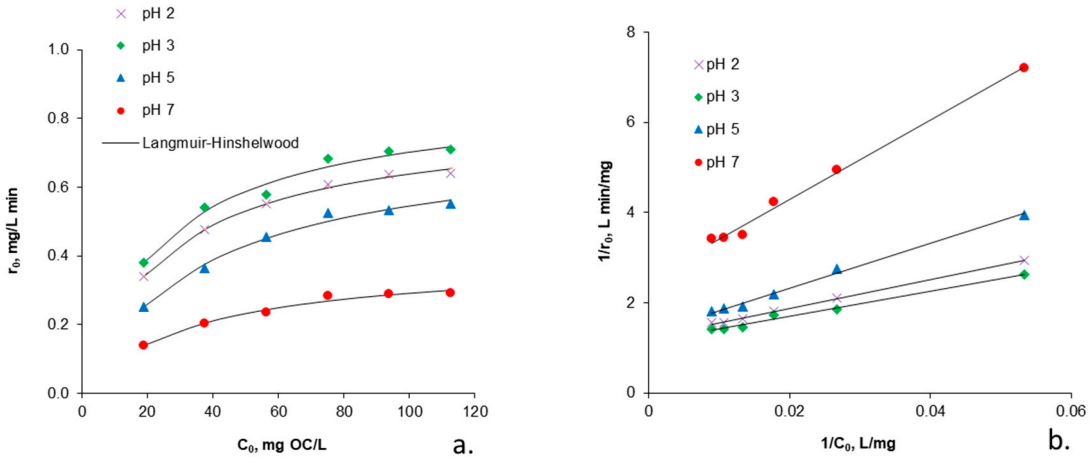

Figure 5. Photocatalytic oxidation kinetics of 2,4-DCF as a function of pH of the working solution: (**a**) non-linear fitting of Langmuir–Hinshelwood kinetics; (**b**) linear fitting of Langmuir–Hinshelwood kinetics; hydrogen peroxide/chlorophenol molar ratio (N) of 1.

Table 4. Kinetic parameters derived from Langmuir–Hinshelwood model for photocatalytic oxidation of 2,4-DCF from aqueous solutions with different pH values; hydrogen peroxide/chlorophenol molar ratio (N) of 1.

pH	k (mg/L·min)	K (L/mg)
2	0.804	0.039
3	0.872	0.041
5	0.748	0.029
7	0.393	0.027

From the data presented in Table 4 it is observed that the photocatalytic oxidation of 2,4-DCF takes place at a faster rate with the increasing of acidity of the working solution with a maximum corresponding to pH 3. The rate constant of the photocatalytic oxidation process (k) is about twice as high at pH 3 comparative with pH 7, and the adsorption constant (K) is about 1.4 times higher at pH 3 compared to that corresponding to pH 7. These results are consistent with the results obtained in the adsorption study in the absence of UV radiation (dark adsorption experiments), which confirms that at low pH values of the working solution the adsorption capacity of the catalyst is higher. Figure 6 shows that complete mineralization of 2,4-dichlorophenol at an initial concentration of 34.6 mg/L is reached after about 4 h if the working solution has a pH of 3 and after 6 h if the working solution has a pH of 7. If the working solution has a concentration of 112.5 mg/L the time required for complete mineralization of the organic substrate exceeds 9 h in the case of the solution with pH 3 and 17 h in the case of solution with pH 7.

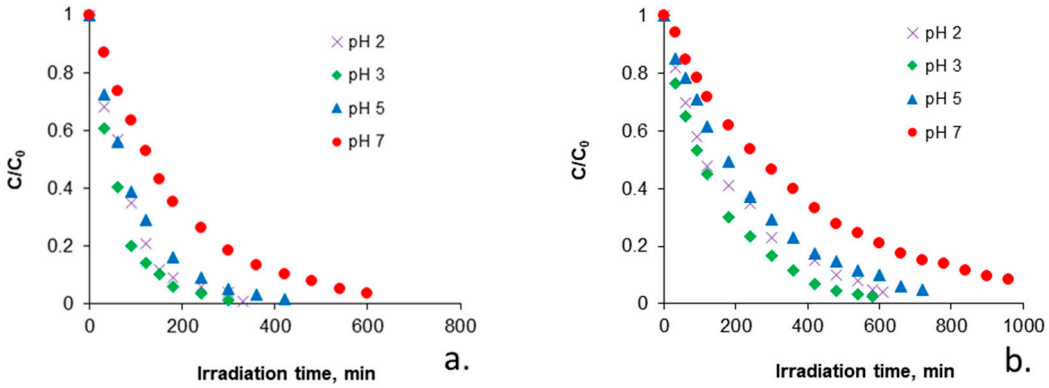

Figure 6. pH effect on the photocatalytic degradation of 2,4-DCF: (**a**) 18.75 mg OC/L; (**b**) 112.5 mg OC/L; hydrogen peroxide/chlorophenol molar ratio (N) of 1.

3.2.2. Influence of Hydrogen Peroxide/Organic Carbon Molar Ratio

The initial rates were plotted as a function to the initial concentration of the organic carbon (Figure 7a) for the three hydrogen peroxide/organic carbon molar ratios used (N 0.5, N 1, and N 2) and at a pH of working solution of 3. The values of the kinetic parameters are presented in Table 5. As can be seen, the rate constant of the photocatalytic oxidation process (k) is about 1.2 higher at the molar ratio N 1 compared to the molar ratio N 2, and about 1.4 higher compared to the molar ratio N 0.5. The adsorption constant (K) has a value about 1.7 higher at the molar ratio N 1 compared to the molar ratio N 2, and about 2.7 higher compared to the molar ratio N 0.5.

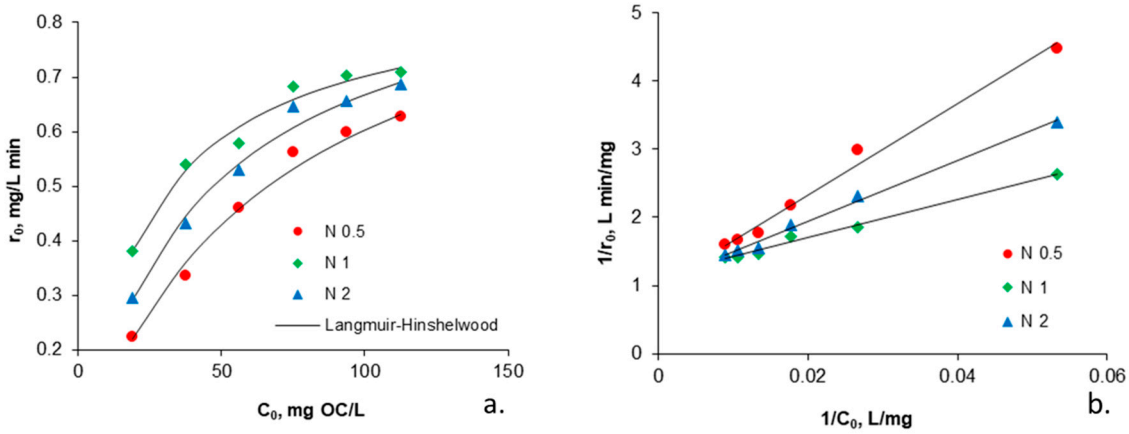

Figure 7. Hydrogen peroxide/organic carbon molar ratios effect on the photocatalytic degradation of 2,4-DCF: (**a**) non-linear fitting of Langmuir–Hinshelwood kinetics; (**b**) linear fitting of Langmuir–Hinshelwood kinetics (pH 3 of working solution).

Table 5. Kinetic parameters derived from Langmuir–Hinshelwood model for photocatalytic oxidation of 2,4-DCF from aqueous solutions with different hydrogen peroxide/organic carbon molar ratios; pH 3 of working solution.

N	k (mg/L·min)	K (L/mg)
0.5	0.613	0.015
1	0.872	0.041
2	0.715	0.024

Figure 8 shows that an almost complete mineralization of the organic substrate at an initial concentration of 34.6 mg OC/L is reached after about 4 h if the hydrogen peroxide/chlorophenol molar ratio (N) is 1, after about 6 h if N is 2, and after about 8 h if N is 0.5. If the working solution has a concentration of 112.5 mg OC/L the time required

for almost complete mineralization of the organic substrate is almost 7 h in the case of hydrogen peroxide/chlorophenol molar ratio (N) of 1, 12 h if N is 2, and 12.5 h if N is 0.5.

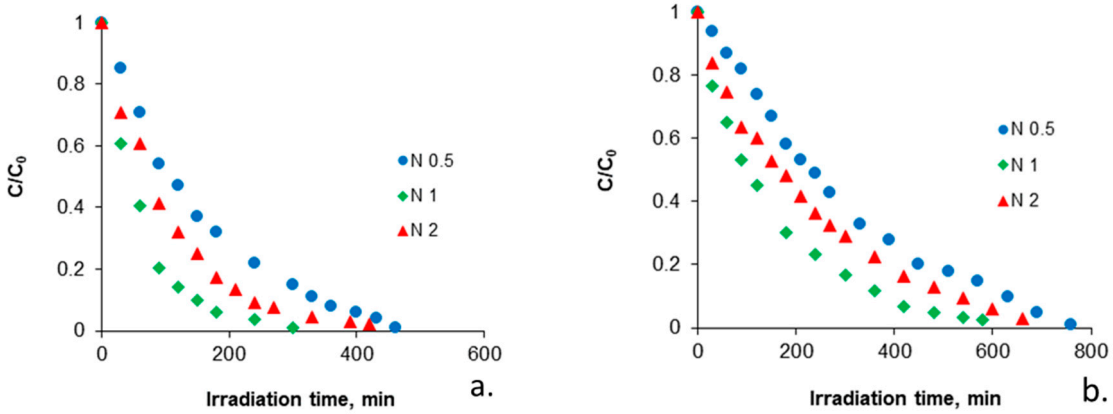

Figure 8. Effect of hydrogen peroxide/organic carbon molar ratio (N) on the photocatalytic degradation of 2,4-DCF: (**a**) 18.75 mg OC/L; (**b**) 112.5 mg OC/L; pH 3 of working solution.

3.2.3. Influence of Initial Concentration of the Organic Carbon

As expected, the initial concentration of the organic substrate influences the rate of photocatalytic degradation. In this respect, it seems that the photocatalytic degradation rate decreases with the increases of initial concentration of the organic substrate (Figure 9a,b). From Figure 9c,d it can be observed that the evolution of photocatalytic degradation in time fits on a pseudo-first-order kinetics (the values of the correlation coefficient R^2 are between 0.9950 and 0.9995) and it is strong depending on the values of the initial concentration of the organic substrate. The apparent rate constant corresponding to the lowest initial organic carbon content is about 3.2 times higher than that corresponding to the highest initial organic carbon content.

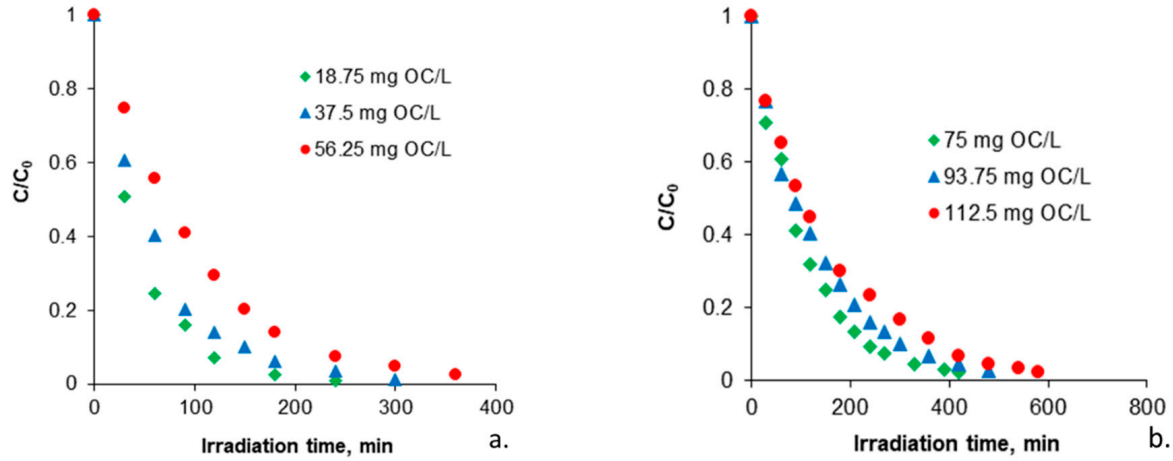

Figure 9. *Cont.*

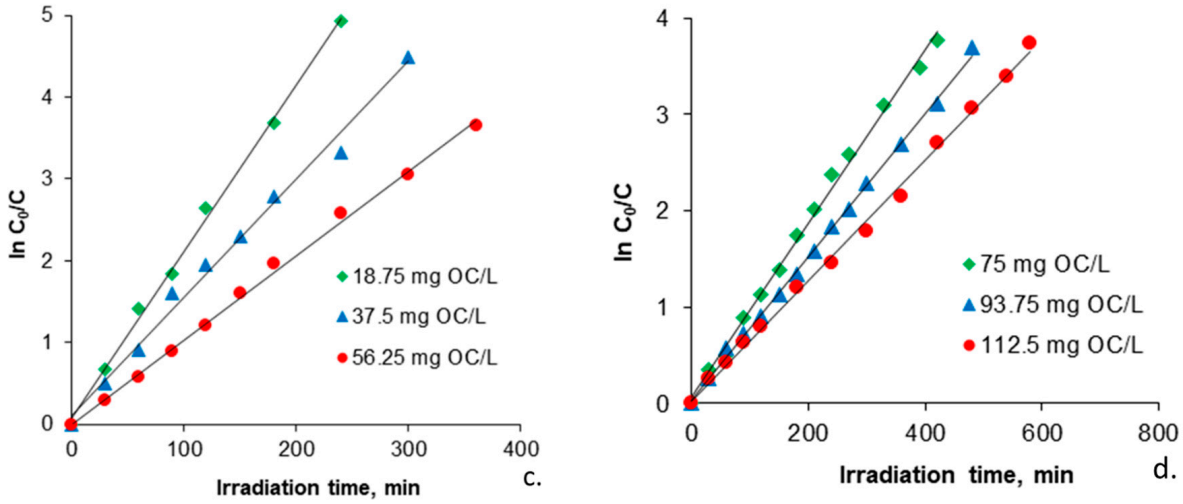

Figure 9. Influence of initial concentration of the organic substrate on its photocatalytic degradation (pH 3 of working solution; hydrogen peroxide/chlorophenol molar ratio N of 1); (**a**,**b**) photocatalytic degradation kinetics; (**c**,**d**) linear fitting of pseudo-first-order kinetics.

4. Discussion

4.1. Influence of pH of the Working Solution

The pH of the aqueous solution containing the organic substrate to be degraded has an important effect on the degradation efficiency, both by modifying the activity of the TiO_2 photocatalyst and by favoring the hydroxyl radical formation reactions. It is considered that the pH value influences the position of the transition band between the conduction band and the valence band of TiO_2 which determines its amphoteric character. It has been determined that around a pH of 7, the catalyst surface is electrically neutral. Below and above this value, the surface of the TiO_2 photocatalyst is charged positively and negatively according to the following equilibria [21]:

$$TiOH_2^+ \rightleftarrows TiOH + H^+ \quad (20)$$

$$TiOH \rightleftarrows TiO^- + H^+ \quad (21)$$

Chlorophenols and their intermediates formed during the photocatalytic degradation process are electronegatively charged compounds or are electrically neutral. This results in better adsorption of organic molecules on the catalyst surface and higher degradation efficiencies at acidic pH values of the solution. The overall photocatalytic reaction can be described by a reaction of the following form [31]:

$$TiO_2\ (\text{photocatalyst}) + OH^- + 2H^+ + O^-{}_2 \rightarrow 3{\cdot}OH + TiO_2\ (\text{photocatalyst}) \quad (22)$$

The equilibrium constant (K_e) for the above reaction has the following form:

$$K_e = \frac{[\cdot OH]^3}{[OH^-]\,[H^+]^2\,[\cdot O_2{}^-]} \quad (23)$$

Considering the ionic product of water:

$$[OH^-]\,[H^+] = K_w = 1 \times 10^{-14} \quad (24)$$

Equation (23) can be written as follows:

$$[\cdot OH]^3 = K_e K_w\,[H^+]\,[\cdot O_2{}^-] \quad (25)$$

From the relation presented above, it is observed that between the concentration of hydrogen ions [H^+] and the concentration of hydroxyl radicals [·OH] there is a direct dependence. Thus, the more acidic the conditions under which the experiment takes place, the more hydroxyl radicals are produced that will degrade the organic substrate faster. This can be highlighted by comparing the kinetic parameters obtained for various pH values of the working solution. However, at pH less than 3, the efficiency of the process decreases due to the protonation effect of hydrogen peroxide with the formation of the oxonium ion ($H_3O_2^+$), which prevents the decomposition of H_2O_2 and thus the formation of ·OH radicals.

The aspects presented above are the basis for the identification of the mechanisms of photocatalytic degradation of 2,4-dichlorophenol. At least two of them could be confirmed by the results obtained in this work. The first one involves the formation of nascent hydrogen (·H) from protons (H^+) adsorbed on the surface of the photocatalyst, which can successively displace chlorine from the benzene ring. Subsequently, the formed phenols can be attacked by hydroxyl radicals (·OH) which can open the benzene ring with the formation of aliphatic compounds. The second one involves a direct attack of the hydroxyl radicals which would lead to the displacement of chlorine from the para position with the formation of 2-chloro-4-hydroxyphenol. Next, there may be a successive attack of the hydroxyl radicals until the benzene ring is open, or there may be a first attack of the nascent hydrogen on the chlorine from the ortho position with the formation of hydroxyquinone followed by the successive attack of hydroxyl radicals until the opening of the benzene ring [9,32]. However, it appears that both degradation mechanisms are strongly influenced by the pH of the aqueous solution, and therefore these are in good agreement with the results found in this work.

4.2. Influence of Hydrogen Peroxide/Organic Carbon Molar Ratio

It is known that the addition of H_2O_2 leads to an improvement in the rate of oxidation of organic compounds due to the formation on the surface of the TiO_2 photocatalyst of HO· radicals, according to the following reaction.

$$TiO_2\left(e^-\right) + H_2O_2 \longrightarrow TiO_2 + OH^- + \cdot OH \quad (26)$$

The rate of degradation of the organic compound increases with increasing concentration of H_2O_2 due to the generation of an increasing number of HO· radicals, the reaction being favored by an acidic pH of the working solution. It has been found that this direct dependence is only valid up to a certain concentration of H_2O_2, after which the reaction rate begins to decrease. This decrease is due to side reactions that occur at the surface of the TiO_2 catalyst, such as the following [33].

$$2H_2O_2 \longrightarrow H_2O + O_2 \quad (27)$$

$$\cdot OH + H_2O_2 \longrightarrow HO_2 \cdot + H_2O \quad (28)$$

$$\cdot OH + HO_2 \cdot \longrightarrow O_2 + H_2O \quad (29)$$

Given that there is a high concentration of H_2O_2 in the system, it will participate in a competition with the organic compound in the reaction with HO· radicals, according to the reaction (28). To avoid these side reactions, the addition of H_2O_2 must be optimized to obtain the maximum rate of degradation of the organic compound. The optimum H_2O_2 concentration depends on the nature and concentration of the organic compound to be degraded. Resulting from the data obtained in this work, a stoichiometric hydrogen peroxide/organic carbon molar ratio is favorable for the degradation of the initial organic compound, namely 2,4-DCF.

4.3. Influence of Initial Concentration of the Organic Carbon

There is an inversely proportional dependence between the initial concentration of organic substrate and the degradation rate. Thus, the higher the initial concentration of organic carbon, the lower the overall degradation rate. This is due to the increasingly intense adsorption of organic substrate molecules on the surface of the photocatalyst as its concentration increases, while the number of hydroxyl radicals formed at constant radiation and constant irradiation time remains constant. Decreasing the ratio between the concentration of the substrate and the concentration of hydroxyl radicals in the solution subjected to irradiation leads to a decrease in the degradation efficiency of the substrate [25]. In the case of this work, this effect is even more visible because the specific surface of the photocatalyst deposited on titanium support is much smaller than if it had been dispersed in the volume of liquid.

5. Conclusions

The results obtained in this paper highlight the importance of operating parameters on the efficiency of removing 2,4-dichlorophenol from aqueous solutions by photocatalytic oxidation in an UV photocatalytic reactor equipped with a TiO_2/stainless-steel photocatalytic membrane. In this respect, it was demonstrated that the photocatalytic degradation rate increases in acidic conditions with a maximum corresponding to pH 3, which leads to an increase in the removal efficiency of 2,4-dichlorophenol. A stoichiometric molar ratio of hydrogen peroxide/organic substrate is favorable for the photocatalytic degradation of 2,4-dichlorofenol. Decreasing or increasing it above the stoichiometric value leads to a significant decrease in the efficiency of photocatalytic degradation of the organic substrate. The rate of photocatalytic degradation decreases with the increasing of initial concentration of 2,4-dichlorophenol. The results obtained showed that there is an inversely proportional dependence between the initial concentration of the organic substrate and the photocatalytic degradation rate.

Author Contributions: Conceptualization, C.O. and L.B.; methodology, C.O. and C.B.; investigation, L.B., G.I.L. and C.B.; writing—original draft preparation, L.B., C.B., G.I.L. and C.O. All authors reviewed and edited the article. All authors have read and agreed to the published version of the manuscript.

Funding: This work was supported by the European Regional Development Fund through Competitiveness Operational Program 2014–2020, Priority axis 1, Project No. P_36_611, MySMIS code 107066, Innovative Technologies for Materials Quality Assurance in Health, Energy and Environmental—Center for Innovative Manufacturing Solutions of Smart Biomaterials and Biomedical Surfaces—INOVABIOMED.

Institutional Review Board Statement: Not applicable.

Informed Consent Statement: Not applicable.

Conflicts of Interest: The authors declare no conflict of interest.

References

1. Yang, Q.; Ma, Y.H.; Chen, F.; Yao, F.B.; Sun, J.; Wang, S.N.; Yi, K.X.; Hou, L.H.; Li, X.M.; Wang, D.B. Recent advances in photo-activated sulfate radical-advanced oxidation process (SR-AOP) for refractory organic pollutants removal in water. *Chem. Eng. J.* **2019**, *378*, 122149. [CrossRef]
2. Tran, N.H.; Reinhard, M.; Gin, K.Y.H. Occurrence and fate of emerging contaminants in municipal wastewater treatment plants from different geographical regions-a review. *Water Res.* **2018**, *133*, 182–207. [CrossRef]
3. Garba, Z.N.; Zhou, W.; Lawan, I.; Xiao, W.; Zhang, M.; Wang, L.; Chen, L.; Yuan, Z. An overview of chlorophenols as contaminants and their removal from wastewater by adsorption: A review. *J. Environ. Manag.* **2019**, *241*, 59–75. [CrossRef] [PubMed]
4. Azizi, E.; Abbasi, F.; Baghapour, M.A.; Shirdareh, M.R.; Shooshtarian, M.R. 4-chlorophenol removal by air lift packed bed bioreactor and its modeling by kinetics and numerical model (artificial neural network). *Sci. Rep.* **2021**, *11*, 670. [CrossRef] [PubMed]

5. Mohammadi, L.; Bazrafshan, E.; Noroozifar, M.; Ansari-Moghaddam, A.; Barahuie, F.; Balarak, D. Removing 2,4-dichlorophenol from aqueous environments by heterogeneous catalytic ozonation using synthesized MgO nanoparticles. *Water Sci. Technol.* **2017**, *76*, 3054–3068. [CrossRef]
6. Ren, H.; Zhan, Y.; Fang, X.; Yu, D. Enhanced catalytic activity and thermal stability of 2,4-dichlorophenol hydroxylase by using microwave irradiation and imidazolium ionic liquid for 2,4-dichlorophenol removal. *RSC Adv.* **2014**, *4*, 62631. [CrossRef]
7. Zhuang, M.; Ren, D.; Guo, H.; Wang, Z.; Zhang, S.; Zhang, X.; Gong, X. Degradation of 2,4-dichlorophenol contaminated soil by ultrasound-enhanced laccase. *Environ. Technol.* **2021**, *42*, 1428–1437. [CrossRef]
8. Poulopoulos, S.G.; Nikolaki, M.; Karampetsos, D.; Philippopoulos, C.J. Photochemical treatment of 2-chlorophenol aqueous solutions using ultraviolet radiation, hydrogen peroxide and photo-Fenton reaction. *J. Hazard. Mater.* **2008**, *153*, 582–587. [CrossRef]
9. Zada, A.; Khan, M.; Khan, A.M.; Khan, O.; Habibi-Yangjeh, A.; Dang, A.; Maqbool, M. Review on the hazardous applications and photodegradation mechanisms of chlorophenols over different photocatalysts. *Environ. Res.* **2021**, *195*, 110742. [CrossRef] [PubMed]
10. Ge, M.; Hu, Z.; Wei, J.; He, Q.; He, Z. Recent advances in persulfate-assisted TiO_2-based photocatalysis for wastewater treatment: Performances, mechanism and perspectives. *J. Alloys Compd.* **2021**, *888*, 161625. [CrossRef]
11. Pelaez, M.; Nolan, N.T.; Pillai, S.C.; Seery, M.K.; Falaras, P.; Kontos, A.G.; Dunlop, P.S.; Hamilton, J.W.; Byrne, J.A.; O'Shea, K. A review on the visible light active titanium dioxide photocatalysts for environmental applications. *Appl. Catal. B Environ.* **2012**, *125*, 331–349. [CrossRef]
12. Ganiyu, S.O.; van Hullebusch, E.D.; Cretin, M.; Esposito, G.; Oturan, M.A. Coupling of membrane filtration and advanced oxidation processes for removal of pharmaceutical residues: A critical review. *Sep. Purif. Technol.* **2015**, *156*, 891–914. [CrossRef]
13. Argurio, P.; Fontananova, E.; Molinari, R.; Drioli, E. Photocatalytic Membranes in Photocatalytic Membrane Reactors. *Processes* **2018**, *6*, 162. [CrossRef]
14. Iglesias, O.; Rivero, M.J.; Urtiaga, A.M.; Ortiz, I. Membrane-based photocatalytic systems for process intensification. *Chem. Eng. J.* **2016**, *305*, 136–148. [CrossRef]
15. Zakria, H.S.; Othman, M.H.D.; Kamaludina, R.; Kadir, S.H.S.A.; Kurniawan, T.A.; Jilani, A. Immobilization techniques of a photocatalyst into and onto a polymer membrane for photocatalytic activity. *RSC Adv.* **2021**, *11*, 6985–7014. [CrossRef]
16. Chong, M.N.; Jin, B.; Chow, C.W.; Saint, C. Recent developments in photocatalytic water treatment technology: A review. *Water Res.* **2010**, *44*, 2997–3027. [CrossRef]
17. Nawawi, W.I.; Zaharudin, R.; Ishak, M.A.M.; Ismail, K.; Zuliahani, A. The Preparation and Characterization of Immobilized TiO_2/PEG by Using DSAT as a Support Binder. *Appl. Sci.* **2017**, *7*, 24. [CrossRef]
18. Leong, S.; Razmjou, A.; Wang, K.; Hapgood, K.; Zhang, X.; Wang, H. TiO_2 based photocatalytic membranes: A review. *J. Membr. Sci.* **2014**, *472*, 167–184. [CrossRef]
19. Molinari, R.; Lavorato, C.; Argurio, P.; Szymański, K.; Darowna, D.; Mozia, S. Overview of Photocatalytic Membrane Reactors in Organic Synthesis, Energy Storage and Environmental Applications. *Catalysts* **2019**, *9*, 239. [CrossRef]
20. Ong, C.S.; Lau, W.J.; Goh, P.S.; Ng, B.C.; Ismail, A.F.; Choo, C.M. The Impacts of Various Operating Conditions on Submerged Membrane Photocatalytic Reactor (SMPR) for Organic Pollutant Separation and Degradation: A Review. *RSC Adv.* **2015**, *5*, 97335–97348. [CrossRef]
21. Dionysiou, D.D.; Suidan, M.T.; Bekou, E.; Baudin, I.; Laîné, J.-M. Effect of ionic strength and hydrogen peroxide on the photocatalytic degradation of 4-chlorobenzoic acid in water. *Appl. Catal. B* **2000**, *26*, 153–171. [CrossRef]
22. Melián, P.E.; Díaz, G.O.; Rodríguez, D.J.M.; Araña, J.; Peña, P.J. Adsorption and photocatalytic degradation of 2,4-dichlorophenol in TiO_2 suspensions. Effect of hydrogen peroxide, sodium peroxodisulphate and ozone. *Appl. Catal. A Gen.* **2013**, *455*, 227–233. [CrossRef]
23. Ai, M.; Qin, W.; Xia, T.; Ye, Y.; Chen, X.; Zhang, P. Photocatalytic Degradation of 2,4-Dichlorophenol by TiO_2 Intercalated Talc Nanocomposite. *Int. J. Photoenergy* **2019**, *2019*, 1540271. [CrossRef]
24. Liu, L.; Chen, F.; Yang, F.; Chen, Y.; Crittenden, J. Photocatalytic degradation of 2,4-dichlorophenol using nanoscale Fe/TiO_2. *Chem. Eng. J.* **2012**, *181–182*, 189–195. [CrossRef]
25. Liu, L.; Chen, F.; Yang, F. Stable photocatalytic activity of immobilized Fe^0/TiO_2/ACF on composite membrane in degradation of 2,4-dichlorophenol. *Sep. Purif. Technol.* **2009**, *70*, 173–178. [CrossRef]
26. Greenberg, A.E.; Clesceri, L.S.; Eaton, A.D. *Standard Methods for the Examination of Water and Wastewater*, 18rd ed.; American Public Health Association, American Water Works Association, Water Environment Federation: Washington, DC, USA, 1992; pp. 5–9.
27. Chen, J.; Xiong, Y.; Duan, M.; Li, X.; Li, J.; Fang, S.; Qin, S.; Zhang, R. Insight into the Synergistic Effect of Adsorption−Photocatalysis for the Removal of Organic Dye Pollutants by Cr-Doped ZnO. *Langmuir* **2020**, *36*, 520–533. [CrossRef]
28. Azizian, S. Kinetic models of sorption: A theoretical analysis. *J. Colloid Interface Sci.* **2004**, *276*, 47–52. [CrossRef] [PubMed]
29. Kumar, K.V.; Porkodi, K.; Rocha, F. Langmuir–Hinshelwood kinetics—A theoretical study. *Catal. Commun.* **2008**, *9*, 82–84. [CrossRef]
30. Sun, P.; Zhang, J.; Liu, W.; Wang, Q.; Cao, W. Modification to L-H Kinetics Model and Its Application in the Investigation on Photodegradation of Gaseous Benzene by Nitrogen-Doped TiO_2. *Catalysts* **2018**, *8*, 326. [CrossRef]
31. Fu, J.; Min Ji, M.; Zhao, Y.; Wang, L. Kinetics of aqueous photocatalytic oxidation of fulvic acids in a photocatalysis–ultrafiltration reactor (PUR). *Sep. Purif. Technol.* **2006**, *50*, 107–113. [CrossRef]

32. Bobirică, L.; Bobirică, C.; Orbeci, C. Examination of Photocatalyzed Chlorophenols for Sequential Photocatalytic-Biological Treatment Optimization. *Catalysts* **2020**, *10*, 985. [CrossRef]
33. Pera-Titus, M.; García-Molina, V.; Baños, M.A.; Giménez, J.; Esplugas, S. Degradation of chlorophenols by means of advanced oxidation processes: A general review. *Appl. Catal. B Environ.* **2004**, *47*, 219–256. [CrossRef]